ACS APPLIED MATERIALS & INTERFACES

Research Article

www.acsami.org

Graphene-Wrapped CoS Nanoparticles for High-Capacity Lithium-Ion Storage

Yan Gu, Yi Xu, and Yong Wang*

Department of Chemical Engineering, School of Environmental and Chemical Engineering, Shanghai University, Shangda Road 99, Shanghai, 200444, P. R. China

Supporting Information

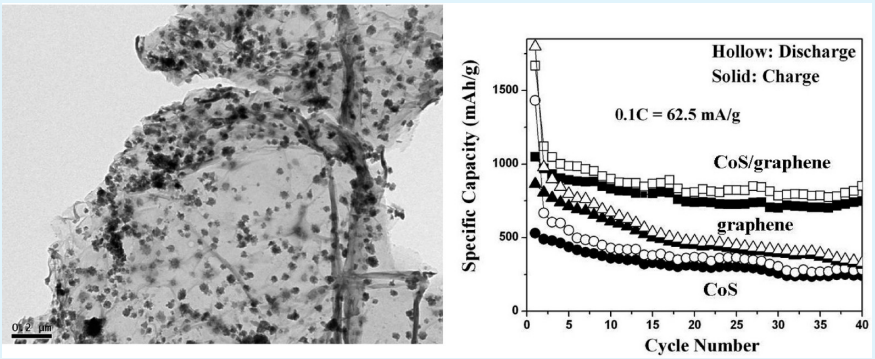

ABSTRACT: Graphene-wrapped CoS nanoparticles are synthesized by a solvothermal approach. The product is significantly different from porous CoS microspheres prepared in the absence of graphene under similar preparation conditions. The CoS microspheres and CoS/graphene composite are fabricated as anode materials for lithium-ion batteries. The CoS/graphene composite is found to be better suitable as an anode in terms of higher capacity and better cycling performances. The nanocomposite exhibits an unprecedented high reversible capacity of 1056 mA h/g among all cobalt sulfide-based anode materials. Good cycling performances are also observed at both small and high current rates.

KEYWORDS: *CoS, graphene nanosheets, nanocomposite, anode, lithium-ion battery*

1. INTRODUCTION

Lithium-ion batteries have been widely applied in portable electronic devices and electric vehicles due to their high energy density and long cycle life.[1−3] Among various anode candidates of lithium-ion batteries, metal sulfides are considered as promising materials because of their high theoretical capacities.[4−8] In particular, cobalt sulfides (CoS, CoS_2, Co_3S_4, Co_9S_8, etc.) have attracted great attention in light of their excellent optical, electrical, and magnetic properties and their applications for lithium-ion batteries.[9−17] Cobalt sulfides particles have been extensively investigated and exhibited Li-ion storage capacities within the range of ∼300−800 mA h/g.[11−14] Recently, more efforts have been paid to other cobalt sulfide morphologies to improve their electrochemical performances. 3D flowerlike CoS displayed a charge (lithium extraction) capacity of ∼850 mA h/g, which decreased to ∼300 mA h/g after 25 cycles.[15] Hollow CoS_2 spheres delivered a high charge capacity of ∼900 mA h/g in the first cycle and 320 mA h/g after 40 cycles.[16] CoS_2@carbon core-shell nanoparticles were also reported with an initial charge capacity of ∼900 mA h/g and the reversible capacity was found to be a high 440 mA h/g after 50 cycles.[17] It is found that fast capacity fading was still a critical problem for these high-capacity cobalt sulfide-based anode materials.

As a new form of carbonaceous material, graphene has attracted tremendous scientific interest in both the fundamental and the applied fields since its discovery in 2004.[18] Graphene possesses intriguing characteristics such as robust structure, high specific surface area, and excellent electronic conductivity. These properties make graphene or graphene-based materials very promising for applications as anode materials for Li-ion batteries.[19−29] To the best of our knowledge, there is no report on the exploration of cobalt sulfide/graphene composite anodes for Li-ion batteries.

Herein, this work reports the facile synthesis of CoS/graphene composite by a solution route and the composite displays an unprecedented high capacity of 1056 mA h/g with good cycling performances at both small and high current rates.

2. EXPERIMENTAL SECTION

2.1. Preparation of CoS and CoS/Graphene Nanocomposites. $CoCl_2{\cdot}6H_2O$,CH_4N_2S, and ethylene glycol (Sinopharm Chemical) were analytical-grade reagents and used as purchased without further purification. Graphene oxide and graphene nanosheets(GNS) were synthesized by a modified Hummers

Received: October 17, 2012
Accepted: January 14, 2013
Published: January 14, 2013

method[30] as reported elsewhere previously,[24] except that graphite nanopowders (XF Nano, 40 nm in thickness) were used as the starting graphite to be exfoliated. In a typical synthesis of CoS/graphene composite, 0.001 mol $CoCl_2 \cdot 6H_2O$ and 0.0022 mol CH_4N_2S were dissolved in 50 mL of ethylene glycol. The precursor solution was magnetically stirred for 0.5 h. Afterwards, 0.08 g graphene oxide was dispersed in the above solution under ultrasonication for 0.5 h. The mixture was transferred into a Teflon-lined autoclave, sealed, and maintained at 180°C for 12 h. After cooling to room temperature naturally, the resulting black solid products were collected after centrifugation, washing with alcohol and drying in vacuum at 60°C for 12 h. The graphene oxide−CoS was further heated at 300 °C in N_2 for 1 h to obtain the final product of the reduced graphene oxide/CoS nanocomposite. For properties comparison, pristine CoS microspheres were prepared following the similar procedure in the absence of graphene oxides.

2.2. Materials Characterizations. The products were characterized by X-ray diffraction (XRD, Rigaku D/max-2550 V, Cu Kα radiation), field-emission scanning electron microscopy (FE-SEM, JSM-6700F) with an energy dispersive X-ray spectrometer (EDS), and transmission electron microscopy/energy dispersive X-ray spectrometer (TEM/EDS, JEOL JEM-200CX and JEM-2010F) in the Instrumental Analysis and Research Center, Shanghai University. The carbon and sulphur elements were measured by a high-frequency infrared carbon-sulphur analyzer (Keguo Instrument, HCS-500P). Raman spectroscopy was recorded on Renishaw in plus laser Raman spectrometer (excitation wavelength, 785 nm; excitation power, 3 mW; spot size, ~1.2 μm). Fourier transform infrared (FT-IR) spectra were collected by a BIO-RAD FTS 135 FT-IR spectrophotometer using the KBr pellet method. The electrical conductivity was measured by a four-electrode method using a conductivity detection meter (Shanghai Fortune Instrument, FZ-2010).

2.3. Electrochemical Measurements. The working electrodes consisted of 80% of the active material, 10% each of the conductive agent (carbon black) and the binder (poly(vinylidene difluoride), PVDF, Aldrich). Lithium foil (China Energy Lithium) was used as counter and reference electrode. The electrolyte was 1 M $LiPF_6$ in a 1:1 w/w mixture of ethylene carbonate (EC) and diethyl carbonate (DEC). Electrochemical measurements were performed on a LAND-CT2001 test system. The Swagelok-type cells were discharged (lithium insertion) and charged (lithium extraction) at a constant current (62.5 mA/g, 0.1C, 1C = 625 mA/g, ~2 mg/cm^2) in 5 mV − 3.0 V. Higher hourly rates (0.5, 1, and 2C) were also used and the first cycle discharging was kept at 0.1C.

3. RESULTS AND DISCUSSION

The crystallographic structures of CoS and CoS/graphene were analyzed by X-ray powder diffraction(XRD) in Figure 1a. A few characteristic (100), (101), (102), and (110) peaks planes could be readily indexed to the standard hexagonal CoS (PDF 65-3418). The characteristic (002) peak of graphitic carbon was very weak indicating that largely disordered carbon structure was obtained in this graphene-based composite. This agrees with previous observations for the chemically derived graphene.[27,28] Figure 1b shows FTIR spectra of graphene oxide, graphene, CoS/graphene. When graphene oxide was transformed into graphene, the peak at 3400 cm^{-1} disappeared which was attributed to the O−H stretching vibration of adsorbed water molecules and surface OH groups. The other O-containing stretches, such as C═O stretch at 1721 cm^{-1}, were also disappeared in graphene and CoS/graphene composite. Figure 1c shows the Raman spectra of graphene oxide, graphene, CoS/graphene. The D/G intensity ratios of graphene oxide and graphene were 1.15 and 1.18, respectively. This ratio was increased to 1.33 for the CoS/graphene composite. The more disordered carbon structure may be ascribed to the partial insertion of CoS nanoparticles into

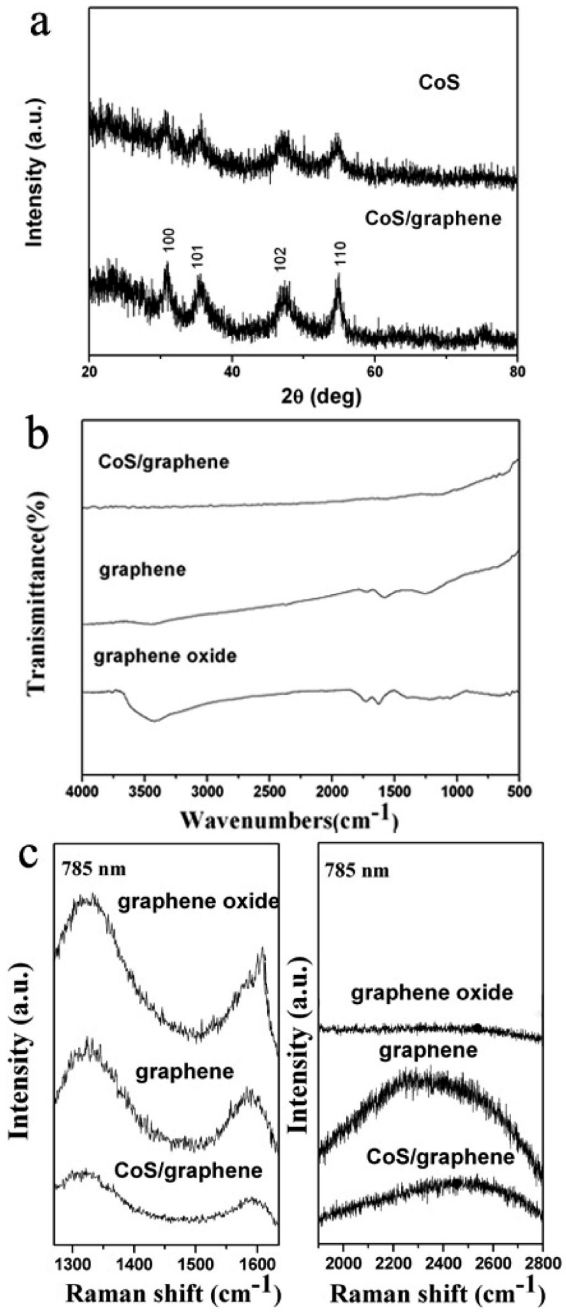

Figure 1. Obtained products: (a) X-ray diffraction patterns; (b) FTIR spectra; (c) Raman spectra.

graphene nanosheets. The 2D peak was also observed in graphene and CoS/graphene.

SEM and TEM images a and b in Figure 2 show graphene nanosheets (GNS) after thermal reduction of graphene oxide materials. Pure graphene nanosheets were wrinkled and quite thin under electron imaging because they consist of only a few carbon layers, which has been described in detail previously.[24] The Pristine CoS microspheres are shown in the SEM and TEM images in Figure 2c and Figure 2d, respectively. These CoS products were ~1−2 micrometers in size and consisted of a number of nanosheets. However, in the presence of graphene oxides supporter, numerous CoS nanoparticles were obtained on GNS surface as shown in the SEM images (Figure 3a and Figure S1 in the Supporting Information) and TEM images (Figure 3b and Figure S2 in the Supporting Information). The

dx.doi.org/10.1021/am3023652 | ACS Appl. Mater. Interfaces 2013, 5, 801−806

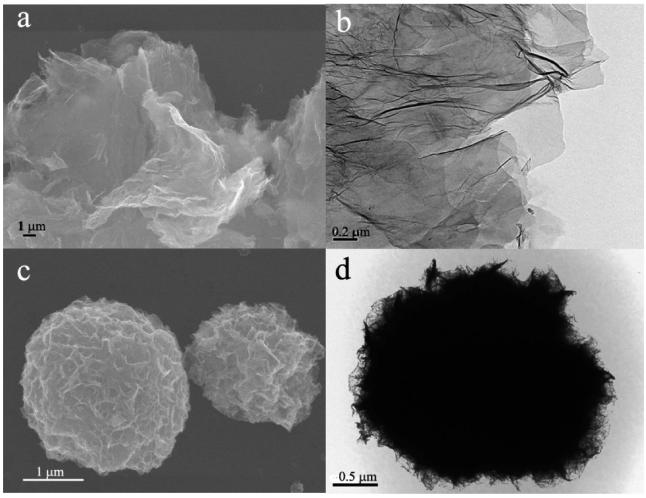

Figure 2. Graphene nanosheets (GNS): (a) SEM image; (b) TEM image. CoS microspheres: (c) SEM image; (d) TEM image.

morphology change from microsphere to nanoparticle should be ascribed to the presence of graphene oxide. As investigated previously,[24] there are still many surface groups on graphene oxide surface, which have critical influence on the nuclei formation and crystal growth of CoS products. These CoS nanoparticles were about 10 nm with uniform particle size distribution. This is also ascribed to the binding effect of graphene oxide, which can hinder the particle aggregation of CoS. The corresponding EDS pattern in Figure 3c confirmed that CoS/graphene composite was composed of three elements of Co, S, and C. The molar ratio of S to Co is around 1:1. The Si element comes from the Si substrate used for SEM characterizations. As indicated by the EDS mapping images (Figure 4) of S, Co, and C elements, these three components were distributed evenly in the composite. The HCS elemental analysis showed that the composite consists of ~76.5 wt % CoS nanoparticles and 23.5 wt % carbon.

Graphene-supported CoS nanoparticles have been reported in a single previous report.[31] A complex step-by-step successive ionic layer absorption and reaction (SILAR) method was used to obtain the composite. In comparison, the solvothermal method used in this work is facile and suitable for large-scale synthesis. Moreover, the obtained CoS nanoparticles are more uniformly dispersed on graphene with smaller particle size and narrower size distribution based on the SEM, TEM, and EDS mapping images results. The facile growth process of uniform CoS nanoparticles/graphene composite is illustrated in Figure 5.

Figures 6a,b show the discharge (lithium insertion) and charge (lithium extraction) curves of CoS and CoS/graphene composite at a current density of 62.5 mA/g. A plateau at ~1.5 V can be observed for pristine CoS anode, which is ascribed to the lithium intercalation and the formation of Li_xCoS_2.[13,16] When the voltage is further decreased, a large amount of lithium intercalation would finally lead to the reduction of CoS_2 to Co and the formation of Li_2S.[13,16] The plateau is not obvious in the discharge curve for graphene−CoS composite, which is possibly due to the presence of graphene materials. Similar results have been reported for other graphene-based composite anodes.[24,28] Initial charge and discharge capacities were 531 mA h/g and 1433 mA h/g respectively for pristine CoS. The large irreversible capacity loss should be largely ascribed to the

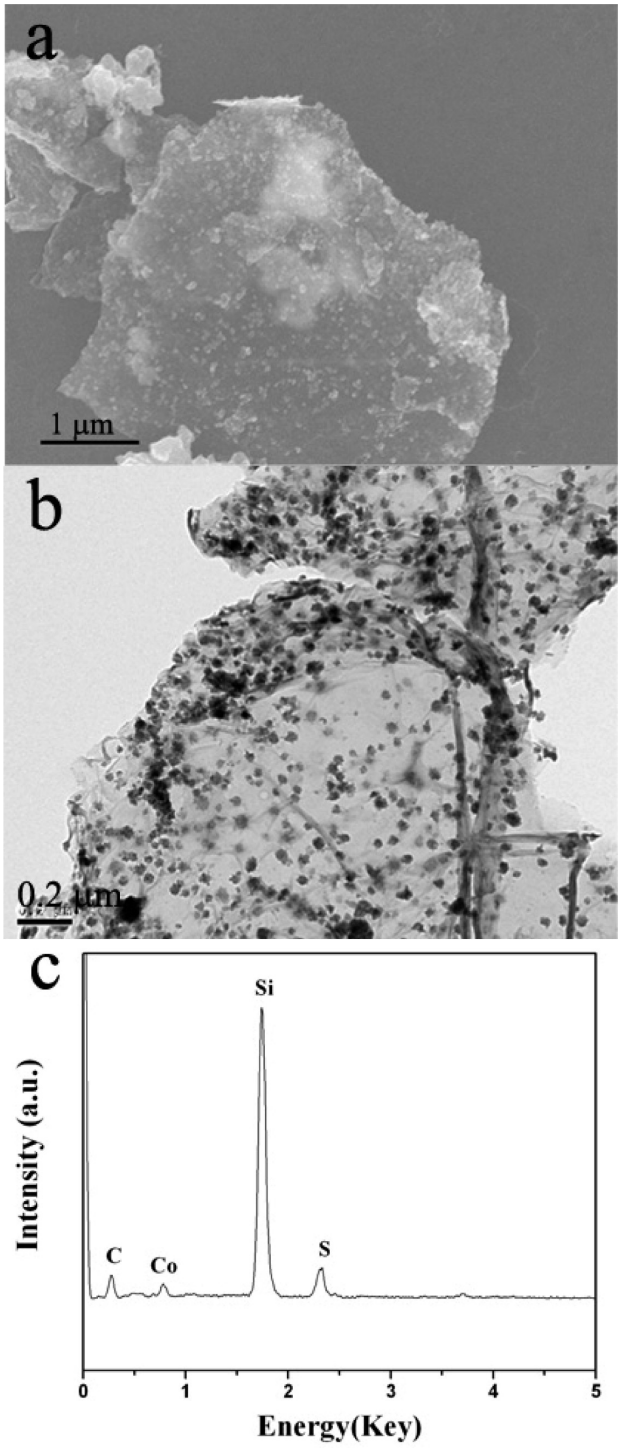

Figure 3. Graphene-wrapped CoS nanoparticles: (a) SEM image; (b) TEM image; (c) EDS pattern of CoS/graphene.

lithium assumption in the formation of solid electrolyte interface (SEI) film on porous CoS microspheres. In comparison, CoS/graphene composite showed initial charge capacity of 1056 mA h/g and discharge capacity of 1669 mA h/g. The reversible charge capacity was larger than the reversible charge capacity of CoS microspheres and the calculated theoretical value of the graphene−CoS composite based on the simple weighted sum of 76.5% CoS (theoretical capacity: 589 mA h/g or the observed capacity for pristine CoS in this work: 531 mA h/g) and 23.5% graphene (theoretical capacity:

dx.doi.org/10.1021/am3023652 | ACS Appl. Mater. Interfaces 2013, 5, 801−806

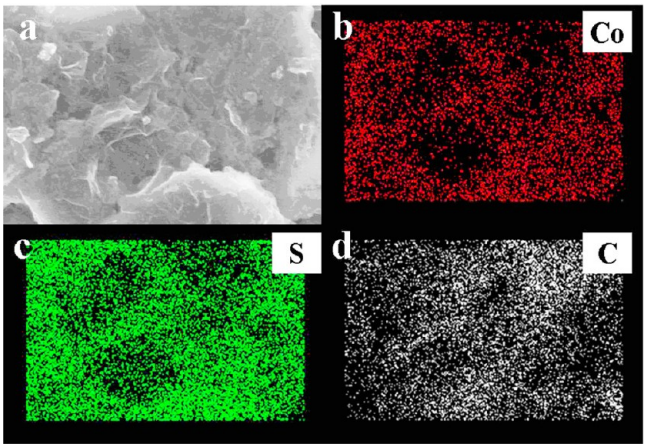

Figure 4. EDS mapping images of S, Co, and C elements in the CoS/graphene composite.

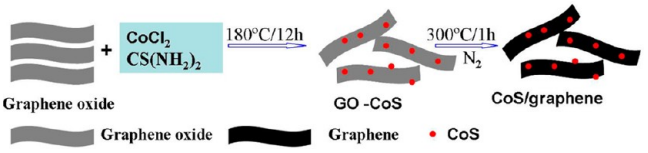

Figure 5. Schematic of the growth process of graphene wrapped CoS nanoparticles.

744 mA h/g or the observed capacity for bare graphene: 864 mA h/g). Therefore an excellent synergetic effect between graphene nanosheets and CoS nanoparticles was observed in the composite. A large extra amount of lithium ion may be stored in the microcavities or pores of disordered graphene-based composite, which is confirmed by the Raman spectra in Figure 1c. This disordered carbon structure should be more apparent by the insertion of CoS nanoparticles into the graphene layers.[24,28] A capacitance effect is also suggested for enhanced Li-ion storage capacity in the graphene-based anodes.[32] A similar higher-than-theoretical capacity was also reported previously for graphene-Sn composite anodes.[27]

The cycling performances of CoS/graphene composite are compared with bare graphene and pristine CoS microspheres in Figure 6c at a current of 62.5 mA/g. The initial charge capacity of graphene was 864 mA h/g, which decreased to 314 mA h/g after 40 cycles. Pristine CoS displayed an initial reversible capacity of 531 mA h/g, which decreased by 54.6% to 241 mA h/g after 40 cycles. In comparison, CoS/graphene showed substantially improved cycliability. A large charge capacity of 749 mA h/g was retained after 40 cycles. This is also a substantial improvement compared to various cobalt sulfides anodes reported previously.[10−17] In particular, a smaller capacity of ∼450 mAh /g could be achieved after same cycle numbers for CoS_2-carbon composite anode at a test current of 0.2 mA/cm^2 and voltage window of 50 mV−3 V,[17] although it exhibited an improved cycliability than pristine CoS_2 anode in the absence of carbon. This large capacity (749 mA h/g) after 40 cycles has not been witnessed previously for this class anode materials (CoS_x-based anode materials).[10−17]

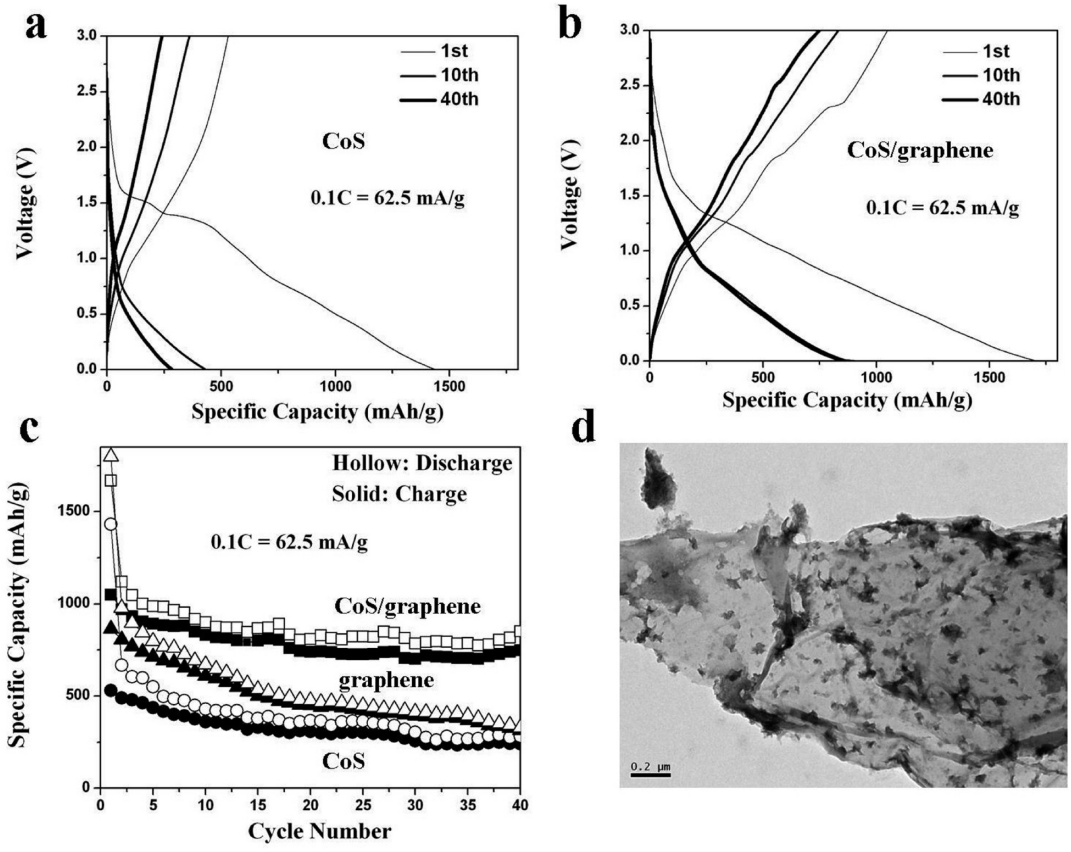

Figure 6. Discharge (lithium insertion) and charge (lithium extraction) curves: (a) CoS and (b) CoS/graphene; (c) cycling performances at 0.1 C; (d) TEM image of the CoS/graphene electrode after 40 cycles.

dx.doi.org/10.1021/am3023652 | ACS Appl. Mater. Interfaces 2013, 5, 801−806

To elucidate the complementary effect of the composite, Figure 6d shows the TEM image of CoS/graphene after repetitive 40 cycles of discharging and charging. There was no detectable particle size growth and particle agglomeration of CoS nanoparticles in the cycled electrode materials. It is suggested that GNS can bind these nanoparticles and prevent their particle agglomeration. On the other hand, CoS particles were evenly distributed between graphene layers, which can effectively prevent the agglomeration or restacking of GNS to common graphite platelets. The heave agglomeration of GNS may result in the loss of their intriguing properties such as mechanical stability, high electrical conductivity and large active surface areas, which are desired in the CoS/graphene composite anode. The electrical conductivity of CoS with and without graphene supporter was measured by a four-electrode technique using a conductivity detection meter. Because of the presence of GNS in the composite, the electrical conductivity of CoS/graphene composite was found to be 1.5 S/cm, which is 6 fold as large as the value of pristine CoS (0.25 S/cm). Therefore the composite also showed a good high-rate capacity and high-rate cycling performances as shown in Figure 7a,b. For

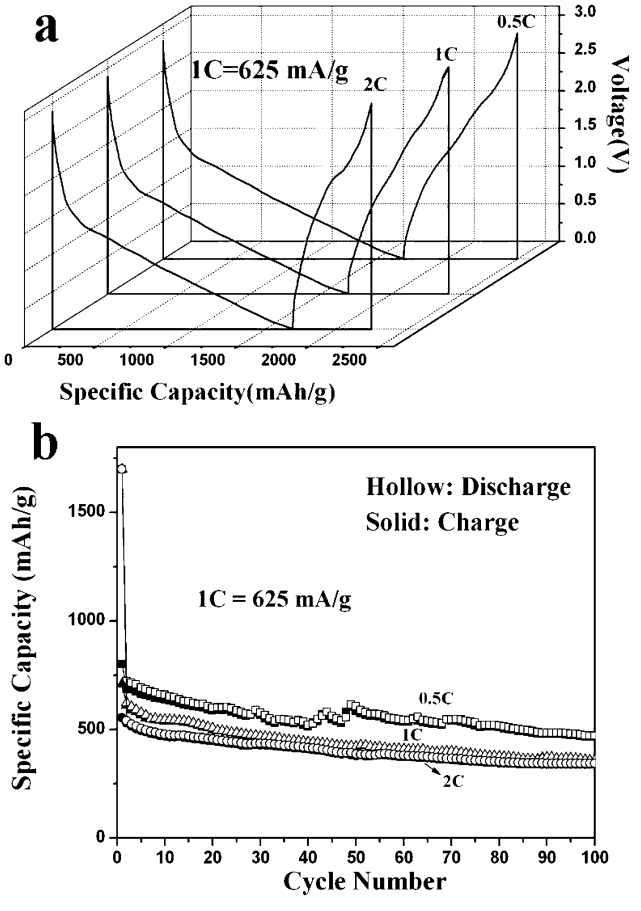

Figure 7. (a) First-cycle discharge and charge curves at large currents; (b) high-rate cycling performances of CoS/graphene.

example, A large reversible capacity of 555 mA h/g could be achieved for the composite at a large current rate of 2C (1250 mA/g). Notably, there was no substantial capacity fading during 100 cycles when the current was increased from 1C to 2C.

4. CONCLUSIONS

In summary, CoS microspheres and graphene wrapped CoS nanoparticles were fabricated in this work. The CoS/graphene composite was found to be more suitable for reversible lithium-ion storage. It showed a higher-than-theoretical reversible capacity of 1056 mA h/g at 62.5 mA/g with good cycling performances and high-rate capability. These large reversible capacities (1056−749 mA h/g in 40 cycles) are not witnessed previously for this class of anode materials (cobalt sulfide-based anodes).[10−17] These improved electrochemical properties have been largely attributed to the increased mechanical stability and electrical conductivity of CoS by the presence of graphene nanosheets (GNS) and the prevented GNS agglomeration by the separation effect of their surface-decorated CoS nanoparticles.

■ ASSOCIATED CONTENT

Ⓢ Supporting Information

SEM and TEM images showing GNS wrapped CoS nanoparticles. This material is available free of charge via the internet at http://pubs.acs.org.

■ AUTHOR INFORMATION

Corresponding Author

*Phone: +86-21-66137723. Fax: +86-21-66137725. E-mail: yongwang@shu.edu.cn.

Notes

The authors declare no competing financial interest.

■ ACKNOWLEDGMENTS

The authors gratefully acknowledge the Program of Professor Special Appointment (Eastern Scholar), the National Natural Science Foundation of China (51271105), Shanghai Municipal Government (11JC1403900, 11SG38, S30109) for financial support.

■ REFERENCES

(1) Park, C. M.; Kim, J. H.; Kim, H.; Sohn, H. J. *Chem. Soc. Rev.* **2010**, *39*, 3115.
(2) Zhou, Z. Y.; Tian, N.; Li, J. T.; Broadwell, I.; Sun, S. G. *Chem. Soc. Rev.* **2011**, *40*, 4167.
(3) Kaskhedikar, N. A.; Maier, J. *Adv. Mater.* **2009**, *21*, 2664.
(4) Débart, A.; Dupont, L.; Patrice, R.; Tarascon, M. *Solid State Sci.* **2006**, *8*, 640.
(5) Masset, P. J.; Guidotti, R. A. *J. Power Sources* **2008**, *178*, 456.
(6) Feng, Y.; He, T.; Alonso-Vante, N. *Chem. Mater.* **2008**, *20*, 26.
(7) Wang, H.; Liang, Y.; Li, Y.; Da, H. *Angew. Chem., Int. Ed.* **2011**, *50*, 10969.
(8) Zhang, L.; Zhou, L.; Wu, H. B.; Xu, R.; Lou, X. W. *Angew. Chem., Int. Ed.* **2012**, *51*, 7267.
(9) Zhang, L.; Wu, H. B.; Lou, X. W. *Chem. Commun.* **2012**, *48*, 6912.
(10) Zhou, Y.; Wu, C.; Zhang, H.; Wu, X.; Fu, Z. *Electrochim. Acta* **2007**, *52*, 3130.
(11) Wang, J.; Ng, S. H.; Wang, G. X.; Chen, J.; Zhao, L.; Chen, Y.; Liu, H. K. *J. Power Sources* **2006**, *159*, 287.
(12) Kim, Y.; Goodenough, J. B. *J. Phys. Chem. C* **2008**, *112*, 15060.
(13) Yan, J. M.; Huang, H. Z.; Zhang, J.; Liu, Z. J.; Yang, Y. *J. Power Sources* **2005**, *146*, 264.
(14) Song, D.; Wang, Q.; Wang, Y.; Wang, Y.; Han, Y.; Li, L.; Liu, G.; Jiao, L.; Yuan, H. *J. Power Sources* **2010**, *195*, 7462.
(15) Wang, Q.; Jiao, L.; Du, H.; Peng, W.; Han, Y.; Song, D.; Si, Y.; Wang, Y.; Yuan, H. *J. Mater. Chem.* **2011**, *21*, 327.
(16) Wang, Q.; Jiao, L.; Han, Y.; Du, H.; Peng, W.; Huan, Q.; Song, D.; Si, Y.; Wang, Y.; Yuan, H. *J. Phys. Chem. C* **2011**, *115*, 8300.

(17) Luo, W.; Xie, Y.; Wu, C.; Zheng, F. *Nanotechnology* **2008**, *19*, 075602.
(18) Novoselov, K. S.; Geim, A. K.; Morozov, S. V.; Jiang, D.; Zhang, Y.; Dubonos, S. V.; Grigorieva, I. V.; Firsov, A. A. *Science* **2004**, *306*, 666.
(19) Lian, P. C.; Zhu, X. F.; Liang, S. Z.; Li, Z.; Yang, W. S.; Wang, H. H. *Electrochim. Acta* **2010**, *55*, 3909.
(20) Shao, Y.; Wang, J.; Engelhard, M.; Wang, C.; Lin, Y. *J. Mater. Chem.* **2010**, *20*, 743.
(21) Guo, P.; Song, H.; Chen, X. *Electrochem. Commun.* **2009**, *11*, 1320.
(22) Wang, G. X.; Shen, X. P.; Yao, J.; Park, J. *Carbon* **2009**, *47*, 2049.
(23) Wang, C. Y.; Li, D.; Too, C. O.; Wallace, G. G. *Chem. Mater.* **2009**, *21*, 2604.
(24) Zou, Y. Q.; Wang, Y. *Nanoscale* **2011**, *3*, 2615.
(25) He, Y. S.; Bai, D. W.; Yang, X. W.; Chen, J.; Liao, X. Z.; Ma, Z. F. *Electrochem. Commun.* **2010**, *12*, 570.
(26) Yao, J.; Shen, X. P.; Wang, B.; Liu, H. K.; Wang, G. X. *Electrochem. Commun.* **2009**, *11*, 1849.
(27) Zou, Y. Q.; Wang, Y. *ACS Nano* **2011**, *5*, 8108.
(28) Lu, L. Q.; Wang, Y. *Electrochem. Commun.* **2012**, *14*, 82.
(29) Chen, J. S.; Wang, Z.; Dong, X. C.; Chen, P.; Lou, X. W. *Nanoscale* **2011**, *3*, 2158.
(30) Hummers, W. S.; Offeman, R. E. *J. Am. Chem. Soc.* **1958**, *80*, 1339.
(31) Das, S.; Sudhagar, P.; Nagarajan, S.; Ito, E.; Lee, S. Y.; Kang, Y. S.; Choi, W. *Carbon* **2012**, *50*, 4815.
(32) Murugan, A. V.; Muraliganth, T.; Manthiram, A. *Chem. Mater.* **2009**, *21*, 5004.